Article

Alginate/lignin: Antioxidant Activities, Anticancer Activity, Physico-chemistry Characteristics, and Acute Toxicity

Nguyen Xuan Hoan [1], Le Thi Hong Anh [2], Hoang Thai Ha [3,*], and Dang Xuan Cuong [4]

[1] Faculty of Biology and Environment, Ho Chi Minh City University of Food Industry, 140 Le Trong Tan, Tan Phu District, Ho Chi Minh 70000, Vietnam; hoannx@hufi.edu.vn
[2] Faculty of Food Technology, Ho Chi Minh City University of Food Industry, 140 Le Trong Tan, Tan Phu District, Ho Chi Minh 70000, Vietnam; anhlth@hufi.edu.vn
[3] Faculty of Food Technology, Ho Chi Minh City University of Food Industry, 140 Le Trong Tan, Tan Phu District, Ho Chi Minh 70000, Vietnam; haht@hufi.edu.vn
[4] Dept. Science and Technology, Ho Chi Minh City University of Food Industry, 140 Le Trong Tan, Tan Phu District, Ho Chi Minh 70000, Vietnam; cuongdx@hufi.edu.vn
* Correspondence: haht@hufi.edu.vn; Tel.: +84-932.082.199

Abstract: Alginate/lignin is a synthetic polymer rich in the biological activity of great interest. Alginate is extracted from seaweed and lignin is extracted from corn stalks and leaves. Antioxidant activities of alginate/lignin were evaluated such as total antioxidant activity, reducing power activity, DPPH free radical scavenging activity, and α – glucosidase inhibition activity. Anticancer activity was evaluated on four cell lines (Hep G2, fibroblast, MCF-7, and NCI H460). Physico-chemistry characteristics of alginate/lignin were determined through FTIR, DSC, SEM_EDS, SEM_EDS mapping, XRD, XRF, and ^{1}H-NMR. Acute toxicity of alginate/lignin was studied on *Swiss albino* mice. The results showed alginate/lignin possessed antioxidant activity such as total antioxidant activi-ty, reducing power activity, especially, α – glucosidase inhibition activity, and no free radical scavenging activity. Alginate/lignin did not be typical in cancer cell lines. Alginate/lignin existed in a thermally stable regular spherical shape in the investigated thermal region. Some specific functional groups of alginate and lignin did not exist in alginate/lignin crystal. Elements such as C, O, Na, and S were popular in the alginate/lignin structure. LD0 and LD100 of alginate/lignin in mice were 3.91 g/kg and 9.77 g/kg, respectively. Alginate/lignin is the potential for application as pharmaceutical materials, functional foods, and supporting diabetes treatment.

Keywords: antioxidant; anticancer; glucosidase, physico-chemistry characteristics, acute toxicity

1. Introduction

Alginate is a bioactive polymer extracted from brown algae (Phaeophyceae) such as *Sargassum, Laminaria, Tubinaria, Macrocystis*, and *Ascophyllum* grown in tropical and subtropical coasts [1-3]. Alginates exist in seaweed cell walls and play a remarkable role in other fields. For example, food, functional food, pharmaceutical and different industries also in the economy [4,5]. Alginate is composed of basic units of (1→4) α-L-guluronic acid (G) and (1→4) β-D-mannuronic acid (M) [6-8]. The arrangement of M and G in alginate leads to the different structures and activities of alginate, and this depends on the species of seaweed, the season, and the geographical location of the algae. Alginate possesses different bioactivities, for example, antioxidant [9,10], anti-tumour, anti-fungal, neuroprotective, anticancer, and immuno-stimulation [11-13]. In brown algae, *Sargassum* in Vietnam, alginate content is about 16 to 36 (%, wt) of dry algae, and the yield of sargassum seaweed gets about 10,000 kg dry per year.

Lignins belong to the polyphenol group in trees, crops, and plants [14]. They are diverse in biological activities and non-toxic. Different plants have different lignin in terms of structure, com-

Preprints (www.preprints.org) | NOT PEER-REVIEWED | Posted: 16 May 2023 doi:10.20944/preprints202305.1137.v1

position and bioactivity [15]. Lignins show great potential for numerous fields such as food, functional food, pharmaceutical, fertilizer, fodder, and fuel. Lignins are found in a mixture of cellulose, hemicellulose, lignin, and extractives of plants [15-17]. Softwood, herbaceous plants, and hardwood species include 27–32%, 0–40%, and 21–31% lignin, respectively [18]. Lignins have structure types sulfur lignin (kraft and lignosulfonates lignin) and sulfur-free lignin (alkaline and organosolv lignin) [16,17]. Phenolic hydroxyl and sulfur (SO_3^{2-} and HSO_3^-) groups are found in a large amount in kraft and lignosulfonates lignin, respectively. Kraft and lignosulfonates lignin is dissolved in water [18-20]. Organosolv is soluble in organic solvents and insoluble in water. Nitrogen and silicate content in alkaline lignin is more than in other lignins [21-23]. In Vietnam, corn stalks are about 120 – 135 tons/ha/year, and the corn planting area is about 1.1 million hectares.

Alginate and lignin possess diverse biological activities, such as anticancer, antibacterial, and antioxidant. Physico-chemistry properties of alginate and lignin are interesting. Hence, the applications of alginate and lignin in different fields are very diverse, for example, carriers of biologically active ingredients in pharmaceuticals, pharmaceutical materials, food packaging films, drug packaging films, and state-forming agents [2,4,15-17]. The combination of alginate and lignin for forming different biomaterials is of great interest, such as alginate/lignin films. However, the notices on alginate and lignin particles and their properties have not appeared. Today, aging, cancer, lack of medicinal herbs, food, drugs, functional foods, and environmental pollution are existential dangers to humans.

Therefore, the study focused on alginate/lignin characteristics composed of antioxidant activity, anticancer activity, physico-chemistry properties, and acute oral toxicity. Lignin and alginate were extracted from by-products of maize harvest (stalks and leaves) and brown algae processing.

2. Results

2.1. Antioxidant Activities

The total antioxidant activity and reducing power activity of alginate/lignin was 218.73 ± 10.45 mg ascorbic acid equivalent/g DW and 479.62 ± 23.18 mg $FeSO_4$ equivalent/g DW. DPPH free radical scavenging capacity of alginate/lignin got the highest value of 19.75 ± 4.07 (%) and the lowest value of 0.53 ± 0.78 (%), corresponding to the concentration of 2000 (µg alginate/lignin/mL) and 31.3 (µg alginate/lignin/mL), respectively. A positive control (Trolox) possessed the highest value (81.48 ± 3.30, %) and the lowest value (5.20 ± 0.75, %) of DPPH free radical scavenging activity, corresponding to 180 (µg Trolox/mL) and 11.25 (µg Trolox/mL), respectively (Table 1). Alginate/lignin and Trolox got the average value of alginate/lignin which corresponded to 8.39 ± 1.56 (%) and 37.98 ± 1.40 (%), respectively.

Table 1. DPPH free radical scavenging activity of alginate/lignin and Trolox

Sample	Concentration (µg/mL)	DPPH free radical scavenging activity (%)
Alginate/lignin	4000	15.31 ± 1.90
	2000	19.75 ± 4.07
	1000	15.72 ± 1.84
	500	9.59 ± 1.13
	250	4.12 ± 1.03
	125	1.61 ± 0.79
	62.5	0.50 ± 0.96
	31.3	0.53 ± 0.78
Trolox	180	81.48 ± 3.30
	90	52.01 ± 0.44
	45	30.34 ± 1.69
	22.5	20.87 ± 0.83
	11.25	5.20 ± 0.75

Preprints (www.preprints.org) | NOT PEER-REVIEWED | Posted: 16 May 2023 doi:10.20944/preprints202305.1137.v1

α – glucosidase inhibition activity of alginate/lignin was in the range of 27.33 ± 3.62 to 87.62 ± 1.13 (%) with IC50 of 50.56 ± 0.8 (µg/mL). The lowest value and highest value of α – glucosidase inhibition activity corresponded to 27.33 ± 3.62 and 87.62 ± 1.13 (%), respectively, occurring as alginate/lignin content got 15.63 and 250 (µg alginate/lignin /mL), respectively. A positive control of acarbose got α – glucosidase inhibition activity of 65.95 ± 0.72 (%), which corresponded to 1000 (µg acarbose/mL) (Table 2).

Table 2. α – glucosidase inhibition activity of alginate/lignin and acarbose.

Sample	Concentration (µg/mL)	α – glucosidase inhibition activity (%)	IC_{50} (µg/mL)
Alginate/lignin	250	87.62 ± 1.13	50.56 ± 0.8
	125	79.74 ± 3.04	
	62.5	49.55 ± 4.83	
	31.25	32.96 ± 5.07	
	15.63	27.33 ± 3.62	
Acarbose	1000	65.95 ± 0.72	

2.2. Anticancer Activities

Table 3. Anticancer activities of alginate/lignin.

Cancer cell lines	Sample	Concentration (µg/mL)	Cell toxicity (%)
NCl-H460	Alginate/lignin	1000	-5.66 ± 6.33
	H_2O	10%	3.34 ± 7.05
	Camptothecin	0.007	64.93 ± 1.58
Fibroblast	Alginate/lignin	1000	14.80 ± 2.00
	H_2O	10%	6.10 ± 3.24
	Camptothecin	2.5	47.89 ± 2.58
HepG2	Alginate/lignin	1000	3.71 ± 4.35
	H_2O	10%	-5.73 ± 4.70
	Camptothecin	0.07	57.62 ± 2.06
MCF-7	Alginate/lignin	1000	1.76 ± 9.14
	H_2O	10%	-5.57 ± 3.95
	Camptothecin	0.05	53.89 ± 3.28

Alginate/lignin did not exhibit anticancer activity on NCI H460 line. Camptothecin possessed anticancer activity on four cell lines composed of NCl-H460, fibroblast, hepG2, and MCF-7, corresponding to 64.93 ± 1.58, 47.89 ± 2.58, 57.62 ± 2.06, and 53.89 ± 3.28 (%), respectively, at camptothecin concentration of 0.007, 2.5, 0.07, and 0.05 (µg camptothecin/mL), respectively. Alginate/lignin showed anticancer activity on two cell lines of fibroblast (14.80 ± 2.00, %) and HepG2 (3.71 ± 4.35, %) at the concentration of 1000 (µg alginate/lignin /mL) (Table 3).

2.3. Physico-chemistry Characteristics

FTIR spectrum of alginate/lignin exhibited ten peaks composed of 1610.56, 1417.68, 1041.56, 877.61, 837.11, 623.01, 435.91, 418.55, 406.98 cm^{-1}, corresponding to the functional groups of C=C, O-H, S=O, C-H, C-S, and oxide groups (Figure 1). Alginate/lignin was crystalized at about 100 °C and melted for continuous degradation at 151.5 °C. The region of melting temperature (T_m) of alginate/lignin was in the range of 148.8 to 159.9 °C with an area of – 276.3 J/g (Figure 2). The structure of alginate/lignin did not exist in a linear or branched chain but crystallographic characteristics (Figure 3a). Alginate/lignin was found in the shape of spherical particles and not broken (Figure 4a). The chemical composition of alginate/lignin focused on the range of 1 to 3 and 21 – 22 keV (Figure 3b) when analysis

Preprints (www.preprints.org) | NOT PEER-REVIEWED | Posted: 16 May 2023 doi:10.20944/preprints202305.1137.v1

of them was by XRF spectrum. CK_a, OK_a, NaK_a, SK_a, and SK_b of alginate/lignin occurred in the energy range under 03 keV (Figure 4b). The results of SEM_EDS mapping presented the mass percentage of elements C, O, Na, and S of alginate/lignin corresponding to 22.16 ± 0.08, 41.55 ± 0.13, 27.62 ± 0.12, 8.66 ± 0.08 (%), respectively. The atom percentage of elements C, O, Na, and S of alginate/lignin got 31.2 ± 0.11, 43.91 ± 0.13, 20.32 ± 0.09, 4.57 ± 0.04 (%), respectively (Table S1).

Figure 1. FTIR spectrum of alginate/lignin

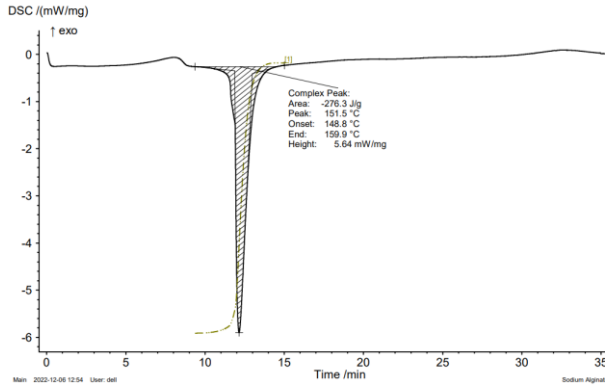

Figure 2. DSC spectrum of alginate/lignin

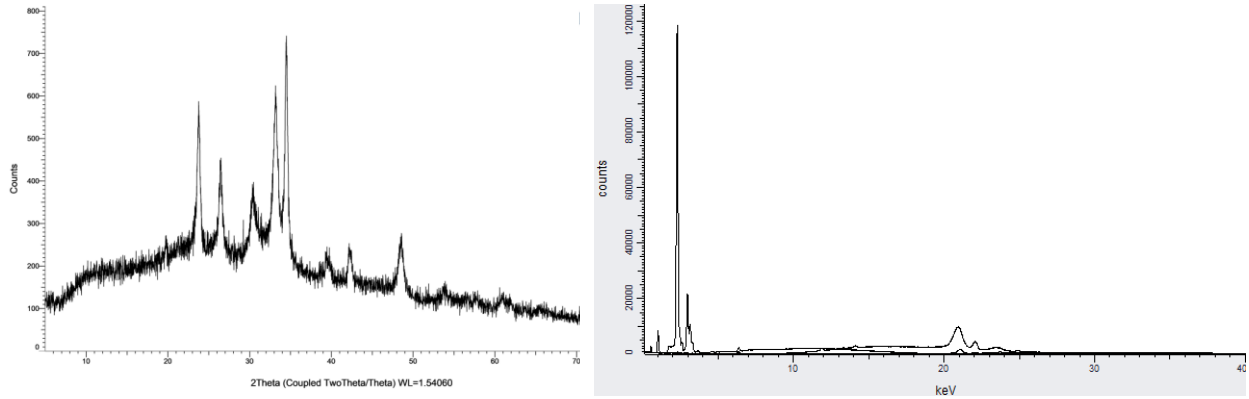

Figure 3. Crystallographic characteristics of alginate/lignin: **(a)** XRD spectrum; **(b)** XRF spectrum.

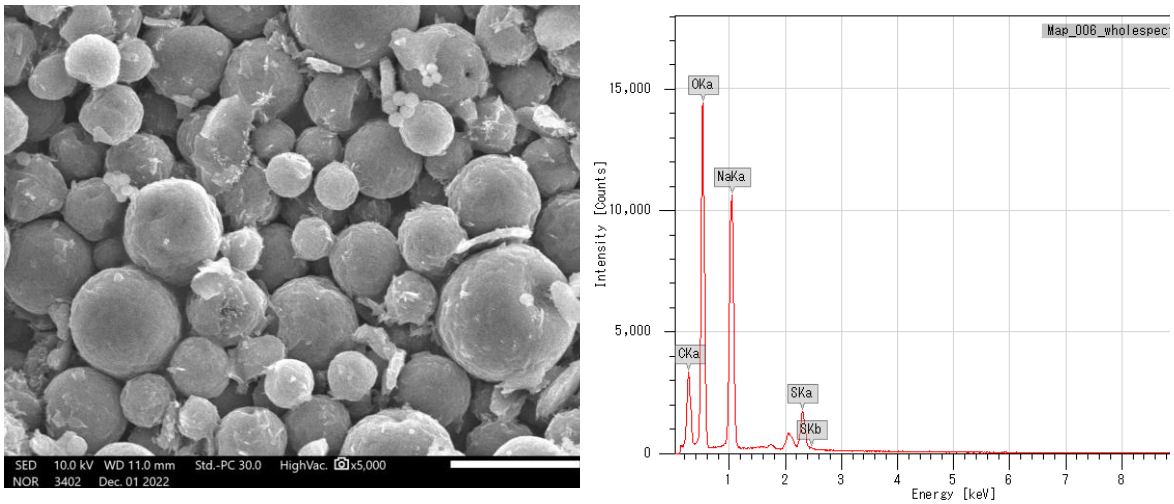

Figure 4. Surface morphology and elemental composition of alginate/lignin: **(a)** SEM_EDS; **(b)** SEM_EDS mapping.

Eight metals were detected in alginate/lignin composed of Si, Ta, Fe, Mg, Na, Na, K, R/R0, and P. Content of eight metals got a value from 0.1 to 54.9%, corresponding to Ta and Na, respectively. Nineteen oxides of alginate/lignin were shown including to SiO2 P_2O_5, SO_3, K_2O, Fe_2O_3, CoO, NiO, ZnO, As_2O_3, SrO, Sb_2O_3, CdO, SnO_2, HfO_2, Ta_2O_5, WO_3, and PbO. The oxide of SO_3 reached the highest

Preprints (www.preprints.org) | NOT PEER-REVIEWED | Posted: 16 May 2023 doi:10.20944/preprints202305.1137.v1

value in the detected oxide of alginate/lignin, in fact, 43.74 (%). CoO, NiO, ZnO, As_2O_3, Sb_2O_3, and SnO_2 got the lowest value (0.01%) in the oxide that was determined in alginate/lignin (Table 4).

Table 4. Composition and content of metal and oxide in alginate/lignin

Metal of alginate/lignin	Content (%)	Oxide of alginate/lignin	Content (%)	Oxide of alginate/lignin	Content (%)
Si	3.50	SiO_2	2.10	SrO	0.03
Ta	0.10	P_2O_5	1.23	Sb_2O_3	0.01
Fe	0.20	SO_3	43.74	CdO	0.02
Mg	0.70	K_2O	0.21	SnO_2	0.01
Na	54.90	Fe_2O_3	0.12	HfO_2	0.02
K	0.50	CoO	0.01	Ta_2O_5	0.03
R/R0	11.50	NiO	0.01	WO_3	0.03
P	1.00	ZnO	0.01	PbO	0.02
		As_2O_3	0.01	Bi_2O_3	0.02
				Na_2O	51.8

The ^{1}H-NMR spectrum of alginate/lignin gave signals at 0.852, 1.068, 1.158, 1.238, 1.361, and 1.535 ppm (Figure 5) with DMSO solvent for running spectrum. The solvent peak presented in the signal at 2.5 ppm.

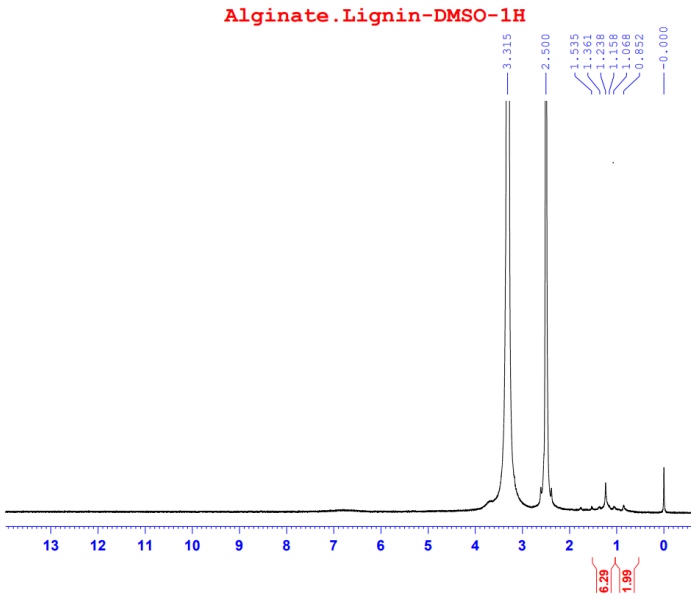

Figure 5. ^{1}H spectrum of alginate/lignin.

2.4. Acute Toxicity

Acute oral toxicity of alginate/lignin material in mice showed that LD_0 and LD_{100} were 3.91 g/kg and 9.77 g/kg, respectively.

$y = 3.6118x^2 - 31.536x + 67.966$; $R^2 = 0.9694$, (1)

From Figure 6 and Equation 1, LD_{16} and LD_{84} were determined 6.67 g/kg and 8.91 g/kg, respectively.

Normal distribution: $S = \frac{LD_{84} - LD_{16}}{2} = \frac{8.91 - 6.67}{2} = 1.12$, (2)

Preprints (www.preprints.org) | NOT PEER-REVIEWED | Posted: 16 May 2023 doi:10.20944/preprints202305.1137.v1

The standard error of LD_{50} was calculated by the formula:

$$SE_{LD50} = \sqrt[2]{\frac{k \times S \times d}{n}} = \sqrt[2]{\frac{0.66 \times 1.12 \times 0.98}{7}} = 0.32, \quad (3)$$

In there: k = 0.66: constant Behrens; S: Normal distribution; d: Dose jump between 2 doses LD_{50}, $d = D_2 - D_1 = 8.79 - 7.81 = 0.98$ g/kg; n: Average number of tested mice in 2 batches near the dose LD_{50}, $n = \frac{6+8}{2} = 7$ mice.

Hence, LD_{50} of material alginate/lignin = 8.15 ± 0.32 (g/kg).

Table 5. Number of dead/lived mice in each batch of alginate/lignin

Dosage (g/kg)	Actual number			Cumulative amount				Mice have diarrhea	
	Deaths	Lives	Total	Deaths	Lives	Total	% deaths	Quantity	Recovery time (hours)
3.91	0	6	6	0	17	17	0.00	2	8 - 10
5.86	1	5	6	1	11	12	8.33	3	12 - 15
7.81	2	4	6	3	6	9	33.33	4	12 - 18
8.79	6	2	8	9	2	11	81.82	8	12 - 24
9.77	6	0	6	15	0	15	100.00	6	Dead mouse

The cumulative mortality percentage (%) changed according to the non-linear equation of level 2 (Eq. 1) (**Figure 6)**.

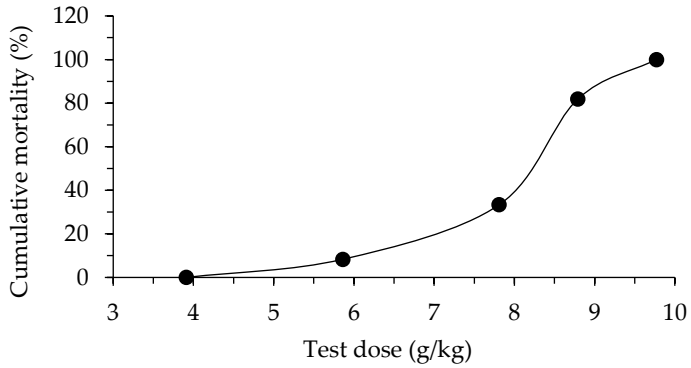

Figure 6. Cumulative mortality by oral dose of alginate/lignin.

3. Discussion

The total antioxidant activity of alginate/lignin was higher than one of alginate in the previous notice [9,10] and polyphenol of sweet rowanberry cultivars [24]. Reducing power activity of alginate/lignin exhibited higher than that of alginate of brow algae *Cystoseira schiffneri* [25]. The total antioxidant activity of alginate/lignin exhibited alginate/lignin possessing antioxidants, and the assay is a pioneer test for further antioxidant assay. Alginates play a role in the absorbent substance for metal, so their reducing power activity is usually high. Alginate/lignin showed the capacity of methylene blue movement [26] and metal in the industry [27]. Reducing power activity is necessary for numerous applications of alginate/lignin. DPPH free radical scavenging activity of alginate/lignin in the current study was higher than one in the notice [28]. The highest DPPH free radical scavenging activity of alginate/lignin only corresponded to Trolox at 22.5 µg/mL. DPPH free radical scavenging efficiency of alginate/lignin is only 1% of that of Trolox. α – glucosidase inhibition activity of alginate/lignin was ten times more than acarbose. The results were potential in the application of diabetes medicine, functional food, or pharmaceutical raw materials. The results of α – glucosidase inhibition activity in the current study showed higher than previous notices on benzoylphloroglucinols from *Garcinia schomburgakiana* [29] and flavonoids [30]. Antioxidant activities in the current study were not found in previous publications.

The results on the anticancer activity of alginate/lignin showed that alginate/lignin was non-selective on tested cancer cells because the inhibition percentage of cancer cells is lower than that of

Preprints (www.preprints.org) | NOT PEER-REVIEWED | Posted: 16 May 2023 doi:10.20944/preprints202305.1137.v1

fibroblast cells. Alginate/lignin did not have potential in the research and development of K treatment products.

Functional groups of alginate and lignin did not found in the structure of alginate/lignin. Alginate/lignin only contained functional groups belonging to peaks of 1610.56 to 406.98 cm^{-1}. Peaks of 435.91, 418.55, and 406.98 cm^{-1} showed the presentation of oxide groups in alginate/lignin. Peak 1417.68 cm^{-1} exhibited the bending of carboxylic acid. The strong stretching of the C-O group got a peak of 1041.56 cm^{-1}. The strong bending of the C=C group presented at a peak of 837.11 cm^{-1} [31,32]. The peak at 1610.56 and 877.61 cm^{-1} represented the tensile vibration of the group - COO- and the oscillation of the glycoside ring in the alginate structure, respectively. The peak at 837.11 cm^{-1} was typical for the aromatic ring vibration of lignin. The disappearance of the characteristic peaks of each starting material was also found, such as the peak of the -COOH group in alginate at about 1738 cm^{-1} lost. Some typical peaks of lignin disappeared, such as the typical band for the symmetric and asymmetrical vibrations of the CH_3 group at 2920 and 2850 cm^{-1}, respectively, and the characterized peak for the C=C oscillation in the aromatic ring at about 1510 and 1460 cm^{-1} [33]. The band disappearance is exhibited by the interaction of two materials to form a stable composite system. DSC spectrum of alginate/lignin showed the melting temperature was similar to lignin in the notice [34,35]. SEM_EDS, SEM_EDS mapping, XRD, and XRF have shown the morphology, elemental distribution, and content of metal and oxide. Some flattened flakes are observed, which may be the beginning materials that were decomposed/torn and not attached to the composite system. Synthetic Alginate/lignin particles have a perfect spherical structure. The spheres are unequal in size, intertwined, and stick together. The XRD spectrum of the Alginate/lignin system shows the formation of a crystalline phase with sharp and sharp peaks on the amorphous background. In previous studies, the XRD spectra of alginate and lignin often show broad peaks of the carbon system, which are typical for the amorphous or poor crystalline structure of the materials [36,37]. The combination of alginate and lignin forms a composite system with the enhancement of the crystalline phase on an amorphous substrate. Based on these results, can completely guide the application of alginate/lignin as pharmaceutical materials and functional foods. The structural properties of alginate/lignin are necessary continuously studied by other solvent systems.

In, LD_0 and LD_{100} is the highest doses that do not cause death in test mice, and the lowest dose causes 100% death in experimental mice of alginate/lignin material. The lethal dose of 50% of the test mice (LD_{50}) is shown in Table 5 and the mice were tested over 3 dose levels with 6 to 8 mice (50% male, 50% female) per dose. After drinking alginate/lignin for 30-45 minutes, the mice decreased their activity, lay still, and had diarrhea. Some mice had severe diarrhea, weak breathing and died within 2-4 hours. The proportion of mice with diarrhea was proportional to the oral dose (Table 5). The surviving mice recovered, and diarrhea stopped after 8-24 hours of drinking the sample. These mice eat bran pellets and drink water normally. Their stool, urine, and weight were not unusual after recovery. Abnormalities in circulatory function, digestive, sensory reflexes, excretory status, and hair of mice were absent. Mice lived within the first 72 h of observation and for 14 days of follow-up. The recovery time was proportional to the test dose level. Died mice during the observation period were operated on for further studies. For example, macroscopic examination showed that the internal organs and organs (heart, lungs, liver, stomach, intestines) were not abnormal. The alginate/lignin material exhibited acute oral toxicity in mice with an LD_{50} value of 8.15 ± 0.32 g/kg, corresponding to an oral dose of 55 kg average adult of 36.443 ± 1.43 g /day (the dose conversion factor between adults and mice is 12.3). After taking alginate/lignin material, some mice showed diarrhea and decreased activity after 30-45 minutes; no abnormalities in circulation and sensory reflexes; then the mouse died within 2-4 hours.

 doi:10.20944/preprints202305.1137.v1

4. Materials and Methods

4.1. Sample preparation

4.1.1. Extraction of Sodium Alginate

Brown seaweed *Sargassum polycystum* was selected, cleaned, and stored below 10 °C during transportation to the laboratory. Salt and impurities of seaweed were removed with fresh water in the laboratory and dried to a moisture content of 19±1%. After that, the seaweed is ground into a fine powder and stored at 10 °C for further studies. Phlorotannin was separated out of brown algae by 96% ethanol according to the ratio of 1/10 (w/v). The extraction of fucoidan was by H_2SO_4 solution (pH 2) for 2 hours at 80 °C. After fucoidan extraction, the residue was pressed to separate the liquid for extracting alginate. Alginate was extracted from the residue for 4 hours at 60 °C with the ratio Na_2CO_3 (pH 9)/dried seaweed (40/1, v/w). After that, the mixture was filtered hot to collect the filtrate and added to 10% $CaCl_2$ solution (the ratio of $CaCl_2$ to alginate was 2.0 / 1.0) to form a calcium alginate precipitate. Calcium alginate was washed with distilled water and decolorized with 20-30 mL of chlorine solution (1% chlorine solution/100 g calcium alginate antioxidant) for 30 min, and the movement of residual chlorine was with fresh water. Bleached calcium alginate was converted to alginic acid by solution (pH 2.0). Next, the alginic acid is converted to sodium alginate by dissolving the alginic acid in a Na_2CO_3 solution with a Na_2CO_3-alginic acid ratio of 0.35/1 (w/w). The mixture was filtered to remove the insoluble fraction of Na_2CO_3 solution and precipitated sodium alginate in 40% ethanol. The sodium alginate precipitate was filtered and dried at 50 °C under a vacuum to obtain the sodium alginate dry powder.

4.1.2. Extraction of alkaline lignin

Corn by-products (corn stalks and leaves) were extracted polyphenols and chlorophyll by 96% ethanol and were dried in the aerated shade until the moisture was below 20±1% for ground and storage in breathable solid bags for further studies. Samples were soaked in 4N NaOH at 80 °C for 150 minutes and filtered. The filtrate was adjusted to pH 5 to form a cellulose precipitate, and then collect the filtrate. The filtrate was adjusted to 70% ethanol concentration using 96% ethanol to obtain a hemicellulose precipitate. After the removed hemicellulose, the filtrate was adjusted to pH 2 to collect precipitated lignin. After centrifugation, the lignin precipitate was washed with clean water and dried at 50 °C under vacuum conditions to constant weight.

4.1.3. Preparation of alginate/lignin particles

Alginate/lignin powder was prepared by a spray-drying method. Sodium alginate in section 4.1.2. (5 % w/v) was dissolved in de-ionized water at 80 °C for 30 min with stirring at 500 rpm, followed by lignin addition in section 4.1.3 (2 % w/v, in 0.1 N NaOH) according to the alginate-to-lignin ratio of 90:10 and assimilated at 500 rpm. Tween 80 and tripolyphosphate were, in turn, added to the ultrasound-assisted mixture at the rate of 0.1%, compared with the total content of alginate and lignin. The mixture was continuously homogenized during spray drying. The spray drying was at the condition as follows: a pump speed of 1,500 mL/hour, pressure in the chamber of 0.2 atm, air heating temperature of 180 °C, and outlet temperature of 90 °C. Alginate/lignin powder was sifted and preserved in a sealed aluminum bag for further evaluation, for example, antioxidant activity, anticancer activity, physico-chemistry characteristics, and acute toxicity.

Preprints (www.preprints.org) | NOT PEER-REVIEWED | Posted: 16 May 2023 doi:10.20944/preprints202305.1137.v1

4.2. Determination of Antioxidant Activity

4.2.1. Total Antioxidant Activity

100 µL sample was diluted ten times with distilled water and mixed into solution A (0.6 M H_2SO_4, 28 mM sodium phosphate, and 04 mM ammonium molybdate) for 5 minutes. Then, the mixture incubation was at 95 °C for 90 min, and measured the mixture absorbance at the wavelength of 695 nm. Ascorbic acid was the standard substance [38].

4.2.2. Reducing Power Activity

The determination of reducing power activity was according to the description of Zhu et al. (2002) [39]. 500 µL sample was mixed, in turn, 0.5 mL of phosphate buffer (pH 7.2), 0.2 mL of 1% $K_3[Fe(CN)_6]$, and kept for 20 min at 50 °C. Then, the mixture was, in turn, added to 500 µL of 10% CCl_3COOH, 300 µL distilled water, and 80 µL of 0.1% $FeCl_3$ for vortexing for 5 minutes. The absorbance measurement of the compound was at 655 nm with the $FeSO_4$ standard.

4.2.3. DPPH Free Radical Scavenging Activity

Dilute DPPH in 80% methanol to form 150 µM of DPPH solution and use immediately. Each well on a 96-well plate was, in turn, added to 200 µL of 150 µM DPPH and 25 µL of the sample at different concentrations. Measurement of the optical density (OD) of the compound was at 517 nm for 30 minutes with a jump of 5 minutes/ time. The positive control was Trolox [40].

The percentage calculation of DPPH free radical scavenging activity was by the formula:

$$\mathbf{SC}\% = \left[\mathbf{1} - \frac{\mathbf{OD_t}}{\mathbf{OD_c}}\right]\mathbf{x100}\ (\%), \quad (4)$$

OD_t and OD_c were the optical density of the test sample and the control, respectively, and these OD value have been subtracted the OD value of solution wells of non-contain DPPH. SC_{50} value (test concentration of 50% DPPH free radical scavenger) determined based on a standard curve of optical density values of samples at different concentrations (Using Prism software with multi-parameter nonlinear regression and $R_2 > 0.9$).

4.2.4. α-glucosidase Inhibition Activity

Add 120 µL of sample and 20 µL of α-glucosidase (1 unit/mL) to each well on a 96-well plate to incubate the mixture at 37 °C for 15 min. Then, add 20 µL of 5 mM *p*-nitrophenyl-α-D glucopyranoside solution /well and incubate for 15 minutes at 37 °C. Finish the reaction by adding 80 µL of 0.2 M Na_2CO_3 solution /well. The absorbance measurement of the mixture was at the wavelength of 405 nm, and the positive control was acarbose [41].

The percentage of α-glucosidase inhibition was calculated using the formula:

$$\mathbf{I}\% = \left[\mathbf{1} - \frac{\mathbf{OD_t}}{\mathbf{OD_c}}\right]\mathbf{x100}(\%), \quad (5)$$

OD_t and OD_c were the optical density of the test and control samples, respectively. The OD value of these samples did not include blank OD value (without α-glucosidase). IC50 value (concentration of 50% α-glucosidase inhibitor test substance) was determined based on the standard curve of optical density values of samples at different concentrations (Using Prism software with $R^2 > 0.9$).

Preprints (www.preprints.org) | NOT PEER-REVIEWED | Posted: 16 May 2023 doi:10.20944/preprints202305.1137.v1

4.3. Determination of Anticancer Activity

4.3.1. Cell Culture

The cell line of breast cancer (MCF-7), lung cancer (NCI H460), liver cancer (Hep G2), and fibroblast provided by ATCC (USA), raised cultured in E'MEM medium (MCF-7, NCI H460, fibroblast, and Hep G2) supplemented with L-glutamine (2 mM), HEPES (20 mM), amphotericin B (0.025 µg/mL), penicillin G (100 UI/mL), streptomycin (100 µg/mL), 10% (v/v) serum FBS bovine fetus and incubated at 37 ^{o}C, 5% CO_2.

4.3.2. Investigation of Cancer Cytotoxic Activity by SRB Method

Inoculation of single cells was on 96-well plates at a density of 10^4 cells/well (for HeLa, Hep G2, fibroblast, and MCF-7 cell lines), 7.5x10^3 cells/well (for the NCI H460 line), and 5x10^4 cells/well for the Jurkat cell line. After 24 h of culture, the cell population was incubated with the probe at different concentrations for 48 h. Then, the total protein fixing of test cells was with a cold solution of 50% trichloroacetic acid (Sigma) (Jurkat alone was 70%) and stained with 0.2% sulforhodamine B solution (Sigma). The results read was with an ELISA reader at two wavelengths of 492 nm and 620 nm. The experiments were triplicated and presented the results on mean ± standard deviation.

After obtaining the optical density values at 492 nm and 620 nm (denoted OD_{492} and OD_{620}):

Calculate the value of $OD_{TS} = OD_{492} - OD_{620}$, (6)

Calculate OD_{492} (or OD_{620}) = $OD_{av} - OD_{blank}$, (7)

Calculate the percentage (%) of cytotoxicity according to the formula:

$$\%I = \left[1 - \frac{OD_{ts}}{OD_C}\right] x100\%, \quad (8)$$

With:

OD_{av}: average OD value of the cells well

OD_{blank}: OD value of blank well (no cells)

OD_{TS}: the OD value of the test sample calculated from formulas (1) and (2)

OD_C: OD value of the control specimen calculated from formulas (1) and (2)

IC_{50} was determined using Prism software with regression multi-parameter non-linearity and $R^2 > 0.9$ [42,43].

4.4. Determination of Physico-Chemistry Characteristics

4.4.1. Functional Groups

The sample was measured at a wavelength range from 4000 to 500 cm^{-1} on an IRAffinity-1S of Shimadzu.

4.4.2. Surface Morphology and Elemental Composition

Alginate/lignin was determined on surface morphology and elemental composition by scanning electron microscopy (SEM) and energy dispersive X-ray spectroscopy (EDS) (SEM_EDS) method.

The method SEM_EDS (Scanning electron microscopy (SEM) and energy dispersive X-ray spectroscopy (EDS) mapping method) was used for analyzing the surface morphology and the distribution of elemental components of alginate/lignin.

4.4.3. Crystallographic characteristics

Crystallographic characteristics of alginate/lignin were determined according to the X-ray diffraction (XRD) method on a Brucker D2 Phaser instrument. Sample measurement parameters: Voltage: 30 KV; Current: 10 mA; Tube: Cu tube with 1.54184 [Å]; Detector: Lynxeye (1D mode); 2ϕ angle: 5-80 degrees; Stepsize (step measurement): 0.02 degrees.

Preprints (www.preprints.org) | NOT PEER-REVIEWED | Posted: 16 May 2023 doi:10.20944/preprints202305.1137.v1

The elemental compositions of alginate/lignin were analyzed by X-ray fluorescence (XRF) method on a Brucker S2 PUMA instrument. Sample measurement parameters: Voltage: 20 kV; Current: 100 µA, 2000 mW; Detector: X-Flash Energy; Energy: -958 eV to 40138 eV.

4.4.4. Thermal analysis

Thermal analysis of alginate/lignin was according to the differential scanning calorimetry (DSC) method on a NETZSCH DSC 204F1 Phoenix. The surveyed temperature was 30 ^{o}C/10.0(K/min)/400 ^{o}C and atmosphere of N_2, 40.0 mL/min / N_2, 60.0 mL/min.

4.4.5. NMR spectra

NMR spectra were measured on a Bruker AVANCE Neo 600MHz instrument at 70 °C, using DMSO as solvent and DSS as an internal standard with a water-reduced measurement technique.

4.5. Determination of Acute Toxicity

4.5.1. Test mice

ICR strain white mice (Swiss albino) composed of male and female at six weeks old with a weight of 20 to 26 g, provided by Nha Trang Institute of Vaccines and Medical Biologicals. Mice were healthy without abnormal expression raised in the standard experimental condition for five days. Mice were supplied adequate food and water in the size cages of 25x35x15 cm.

4.5.2. Investigation of Acute Oral Toxicity

Principle: Give the test rats the same dose of the test sample under the same steady-state conditions, and observe the reactions occurring within 72 hours and 14 days.

Procedure: Ten mice were fasted for at least 12 hours before giving them the maximum possible oral dose of the test sample with a volume of 50 ml/kg [44]. Recording the general movement, behavior, hair state, eating, urination, and death of mice was done within 72 hours. If the mouse shows no abnormality or dies after 72 hours, continue monitoring for 14 days. There are three possible cases:

- Case 1: After the mice drank the test sample, the mice did not die, continuously determining the highest possible dose of the test sample through the needle without causing the mouse to die (D_{max}).

- Case 2: After giving the test sample to mice, the mortality rate is 100%, then try with a dose of ½ of the first dose until a minimum amount is lethal to 100% of mice (LD_{100}) and a maximum amount that is not lethal to rats (LD_0). Conduct testing to determine LD_{50}:

Dividing mice into four lots, each batch of 6 mice. Divide the four doses by an exponential interval from LD_0 - LD_{100}. At doses close to LD_{50}, the number of mice was increased for more accurate measurements and monitoring for 72 hours to record the movements of mice, and the number of dead mice in each batch, and calculate the mortality fraction to find LD_{50}.

- Case 3: After giving the test sample, the mouse death rate is lower than 100%, the dose of LD_{100} cannot be determined, and the LD_{50} cannot be determined. In this case, it is only possible the determination of the maximum dose which is not lethal to mice, called sub-lethal dose (LD_0).

The LD_{50} value determined by the Behrens method based on two doses close to the LD_{50} lethal dose:

$$LD_{50} = D_1 + \frac{(50-a)\ x\ d}{b-a}, \quad (9)$$

In which:

D_1 is the lethal dose a% of test animals (dose close to 50%).

D_2 is the deadly dose b% of test animals (the upper dose is close to 50%).

$d = D_2 - D_1$ is the dose step between 2 doses near LD_{50}.

 doi:10.20944/preprints202305.1137.v1

4.6. Data Analysis

Each experiment was triplicated (n=3) and presented the results under mean ± SD. Analysis of ANOVA and statistics were on the software MS. Excel 2010. IC50 determination of cell toxicity activity, DPPH free radical scavenging activity, and α-glucosidase inhibition activity were analyzed using Prism software.

5. Conclusions

Alginate/lignin is a potential antioxidant material for pharmaceutical materials, functional foods, and supporting diabetes treatment. Total antioxidant activity and reducing power activity were highly evaluated in alginate/lignin, especially, α – glucosidase inhibition activity of alginate/lignin. Alginate/lignin did not exhibit DPPH free radical scavenging activity and also be typical in four cancer cell lines such as Hep G2, fibroblast, MCF-7, and NCI H460. Alginate/lignin was in a thermally stable regular spherical shape containing both metal and oxide. C, O, Na, and S were typical elements in the alginate/lignin structure. Alginate/lignin crystal did not contain some specific functional groups of alginate and lignin. The acute toxicity test of alginate/lignin in mice presented LD0 (3.91 g/kg) and LD100 (9.77 g/kg).

Supplementary Materials: The following supporting information can be downloaded at: www.mdpi.com/xxx/s1, Table S1: Mass and atom of elements in alginate/lignin on SEM_EDS mapping.

Author Contributions: Conceptualization, L.T.H.A. and H.T.H.; methodology, N.X.H. and H.T.H.; software, D.X.C.; validation, H.T.H., and N.X.H; formal analysis, H.T.H; investigation, H.T.H. and N.X.H.; resources, L.T.H.A.; data curation, D.X.C.; writing—original draft preparation, L.T.H.A., N.X.H., H.T.H. and D.X.C.; writing—review and editing, L.T.H.A., H.T.H., N.X.H. and D.X.C.; visualization, N.X.H.; supervision, D.X.C.; project administration, N.X.H.; funding acquisition, N.X.H. All authors have read and agreed to the published version of the manuscript.

Funding: This research was funded by the Ministry of Industry and Trade, grant number 114.2021.ĐT.BO/HĐKHCN".

Institutional Review Board Statement: The animal study protocol was approved by the Institutional Review Board of the Ministry of Health (458/QĐ-BYT, February 16, 2012) for studies involving animals.

Informed Consent Statement: Not applicable.

Data Availability Statement: Not applicable.

Acknowledgments: Thankful for Assoc. Prof. Dr. Do Thi Hong Tuoi – Ho Chi Minh City University of Medicine and Pharmacy

Conflicts of Interest: The authors declare no conflict of interest.

References

1. Saji, S.; Hebden, A.; Goswami, P.; Du, C. A brief review on the development of alginate extraction process and its sustainability. *Sustainability* **2022**, *14*, 5181. https://doi.org/10.3390/ su14095181.
2. Roya, A.-k.; Latifa, T.; Nasim, S.; Anil, K.P.; Slim, A.; Philippe, M. Structures, properties and applications of alginates. *Mar Drugs* **2022**, *20*(6), 364; https://doi.org/10.3390/md20060364.
3. Savindra, K.; Dinabandhu, S. A comprehensive analysis of alginate content and biochemical composition of leftover pulp from brown seaweed *Sargassum wightii*. *Algal Res*. **2017**, *23*, 233-239.
4. Vijayalakshmi, K.; Latha, S.; Rose, M.H.; Sudha, P.N. Industrial applications of alginate. In *Industrial applications of marine biopolymers*; Sudha, P.N., Ed.; CRC Press: Boca Raton, FL, USA, 2017; pp. 545–575.
5. Niculescu, A.-G.; Grumezescu, A.M. An up-to-date review of biomaterials application in wound management. *Polymers* **2022**, *14*, 421.
6. Hecht, H.; Srebnik, S. Structural characterization of sodium alginate and calcium alginate. *Biomacromolecules* **2016**, *17*, 2160–2167.

7. Okolie, C.L.; Mason, B.; Mohan, A.; Pitts, N.; Udenigwe, C.C. Extraction technology impacts on the structure-function relationship between sodium alginate extracts and their in vitro prebiotic activity. *Food Biosci* **2020**, *37*, 100672.
8. Thuy, T.T.T.; Thu, T.M.Q.; Van, T.T.T.; Thanh, V.N.; Shiho, S.; Shinichi, K.; Yoshiaki, Y. Structural characteristics and biological activity of different alginate blocks extracted from brown seaweed *Turbinaria ornate*. *J Carbohydr Chem* **2021**, *40*(1-3), 1-18.
9. Dang, X.C.; Dang, T.T.T.; Do, T.K. Biophysical-chemistry characterization of alginate in brown algae species *Sargassum dupplicatum*. *WJFST. Special Issue: Marine bio-polymer: Bio-activity, extraction and application* **2020**, *4*(1), 17-22. doi: 10.11648/j.wjfst.20200401.13.
10. Nguyen, D.T.; Vu, N.B.; Nguyen, X.H.; Dang, T.T.T.; Do, T.K.; Nguyen, K.N.; Nguyen, N.B.H.; Pham, T.T.; Pham, T.T.; Dang, X.C. The content, antioxidant activity, and structural characteristics of sodium alginate extracting from *Sargassum polycystum* grew in Vietnam: Effect of various extraction conditions. *J Pharm Res Int* **2021**, *33*(41A), 197-206.
11. Cör, A.D.; Knez, Ž.; Knez, M.M. Antioxidant, antibacterial, antitumor, antifungal, antiviral, anti-inflammatory, and nevro-protective activity of *Ganoderma lucidum*: An overview. *Front Pharmacol* **2022**, *13*, 934982. doi: 10.3389/fphar.2022.934982.
12. Maochen, X.; Qi, C.; Yu, W.; Han, X.; Jiarui, Z.; Qing, Z.; Aiguo, J.; Shuliang, S. Advances in research on the bioactivity of alginate oligosaccharides. *Mar Drugs* **2020**, *18*(3), 144. doi: 10.3390/md18030144.
13. Jiayu, C.; Yu, H.; Lirong, Z.; Yingjian, W.; Shichao, W.; Yanzi, Z.; Haiyan, G.; Degang, J.; Yingtao, W. Alginate oligosaccharide DP5 exhibits antitumor effects in osteosarcoma patients following surgery. *Front Pharmacol* **2017**, *8*, 623. doi: 10.3389/fphar.2017.00623.
14. Qingquan, L.; Le L.; Luqing, Z. Lignins: Biosynthesis and biological functions in plants. *Int J Mol Sci* **2018**, *19*(2), 335. doi: 10.3390/ijms19020335.
15. Jianming, T.; Sheng, L.; Fayin, Y.; Yun, Z.; Lin, L.; Guohua, Z. Lignin – An underutilized, renewable and valuable material for food industry. *Crit Rev Food Sci Nutr* **2020**, *60*(12), 2011-2033.
16. Atika, A.; Fahriya, P.S.; Asma, S.; Witta, K.R.; Melati, S.; Nurhani, A.; Widya, F.; Adarsh, K. Current roles of lignin for the agroindustry: Applications, challenges, and opportunities. *Int J Biol Macromol* **2023**, *240*, 124523.
17. Theodoros, V.; George, Z.; Francis, V. Plant food residues as a source of nutraceuticals and functional foods. *Foods* **2016**, *5*(4), 88. doi: 10.3390/foods5040088.
18. Ngo, D.V.; Hang, T.T.; Nhi, D.B.; Cuong, D.V.; Hung, V.N. Lignin and cellulose extraction from Vietnam's rice straw using ultrasound-assisted alkaline treatment method. *Int J Polym Sci* **2017**, *2017*, 1-8. https://doi.org/10.1155/2017/1063695.
19. Tarasov, D.; Leitch, M.; Fatehi, P. Lignin–carbohydrate complexes: properties, applications, analyses, and methods of extraction: a review. *Biotechnol Biofuels* **2018**, *11*, 269(2018). https://doi.org/10.1186/s13068-018-1262-1.
20. Jost, R.; Fredrik, H.B.; Gary, C.-C. Functional surfaces, films, and coatings with lignin – a critical review. *RSC Adv* **2023**, *13*, 12529-12553. DOI: 10.1039/D2RA08179B.
21. Pinar, K.; Sansanee, K.; Marco, P.C.M.; Samir, S.; Timothy, D.H.B.; Gary, J.L. Pharmaceutical applications of lignin-derived chemicals and lignin-based materials: linking lignin source and processing with clinical indication. *Biomass Conv Bioref* **2023**. https://doi.org/10.1007/s13399-023-03745-5.
22. Nasrullah, A.; Bhat, A.H.; Sada, K.A.; Ajab, H. 9 - Comprehensive approach on the structure, production, processing, and application of lignin. In *Lignocellulosic fibre and biomass-based composite materials. processing, properties and applications*; Mohammad, J., Paridah, M.T., Naheed, S., Eds.; Woodhead Publishing: Cambridge, United Kingdom, 2017; pp. 165-178.
23. Roland, E.H.; Nicolas, B.; Laurent, C.; Christian, S.; Poulomi, S.; Arthur, R. Characterization of milled wood lignin and ethanol organosolv lignin from miscanthus. *Polym Degrad Stab* **2009**, *94*(10), 1632-1638.
24. Orsavová, J.; Tunde, J.; Růžena, B.; Jiří, M. Total phenolic and total flavonoid content, individual phenolic compounds and antioxi-dant activity in sweet rowanberry cultivars. *Antioxidants* **2023**, *12*(4), 913. https://doi.org/10.3390/antiox12040913.
25. Benslima, A.; Sellimi, S.; Hamdi, M.; Nasri, R.; Jridi, M.; Cot, D.; Suming, L.; Moncef, N.; Zouari, N. The brown seaweed *Cystoseira schiffneri* as a source of sodium alginate: Chemical and structural characterization, and antioxidant activities. *Food Biosci* **2021**, *40*, 100873. doi:10.1016/j.fbio.2020.100873.

26. Tao, C.; Haochen, L.; Jie, G.; Guowen, H.; Yuan, Z.; Xiuqin, T.; Xiaobing, H. Efficient removal of methylene blue by bio-based sodium alginate/lignin composite hydrogel beads. *Polymers* **2022**, *14*(14), 2917; https://doi.org/10.3390/polym14142917.
27. Xiangpeng, G.; Cheng, G.; Junjie, H.; Zhuo, Z.; Hongming, L.; Mingyang, L. Adsorption of heavy metal ions by sodium alginate based adsorbent-a review and new perspectives. *Int J Biol Macromol* **2020**, 164(1), 4423-4434. doi:10.1016/j.ijbiomac.2020.09.046.
28. Rita, A.; Federica, M.; Rodolfo, E.; Gerardino, D.; Lucia, P.; Alessandra, N. Recovery of lignins with potent antioxidant properties from shells of edible nuts by a green ball milling/deep eutectic solvent (des)-based protocol. *Antioxidants* **2022**, *11*(10), 1860. https://doi.org/10.3390/antiox11101860.
29. Huy, T.N.; Thanh-Trung, N.; Thuc-Huy, D.; Nguyen-Minh-An, T.; Chuong, H.N.; Thi-Hong-Anh, N.; Jirapast, S. α-glucosidase inhibitory and antimicrobial benzoylphloroglucinols from *Garcinia schomburgakiana* fruits: In vitro and in silico studies. *Molecules* **2022**, *27*(8), 2574. https://doi.org/10.3390/molecules27082574.
30. Bo-wei, Z.; Xia, L.; Wen-long, S.; Yan, X.; Zhi-long, X.; Chun-lin, Z.; Yue-sheng, D. Dietary flavonoids and acarbose synergistically inhibit α-glucosidase and lower postprandial blood glucose. *J Agric Food Chem* **2017,** *65*(38), 8319–8330.
31. Bin, S.; Hongxu, L.; Ruru, S.; Pai, P.; Yun, J.; Diao, S. Hydrogel synthesis based on lignin/sodium alginate and application in agriculture. *Int J Biol Macromol* **2020**, *144*, 219-230. doi: 10.1016/j.ijbiomac.2019.12.082.
32. Dominika, F.; Zbigniew, H.; Dorota, K. Fabrication, characterization and evaluation of an alginate–lignin composite for rare-earth elements recovery. *Materials (Basel)* **2022**, *15*(3), 944. doi: 10.3390/ma15030944.
33. Guiting, L.; Hongxun, Z.; Hong, W.; Rong, C.; Shaoyun, G. Preparation of alginate hydrogels through solution extrusion and the release behavior of different drugs. *J Biomater Sci Polym Ed* **2016**, *27*(18), 1808-1823.
34. Tong, H.; Nanta, S.; Ayumu, T.; Olena, S.; Pelle, M.; Weihong, Y. Characterization of lignin at pre-pyrolysis temperature to investigate its melting problem. *Fuel* **2019**, *235*, 1061-1069.
35. Keshaw, R.A.; Harit, J. Physico-chemical properties of lignin–alginate based films in the presence of different plasticizers. *Iran Polym J* **2016**, *25*, 661–670.
36. Köhnke, J.; Gierlinger, N.; Prats-Mateu, B.; Unterweger, C.; Solt, P.; Mahler, A.; Schwaiger, E.; Liebner, F.; Gindl-Altmutter, W. Comparison of four technical lignins as a resource for electrically conductive carbon particles. *BioRes* **2019**, *14*(1), 1091-1109.
37. Samer, R.A.; Mutasem, O.T. Enhanced drug encapsulation and extended release profiles of calcium–alginate nanoparticles by using tannic acid as a bridging cross-linking agent. *J Microencapsul* **2015**, 32(1), 96-105.
38. Prieto, P.; Pineda, M.; Aguilar, M. Spectrophotometric quantitation of antioxidant capacity through the formation of a phosphomolybdenum complex: Specific application to the determination of vitamin E. *Anal Biochem*, **1999**, *269*(2), 337-341.
39. Zhu, Q.; Hackman, R.; Ensunsa, J.; Holt, R.; Keen, C. Antioxidative activities of Oolong tea. *J Agric Food Chem* **2002**, *50*(23), 6929-6934.
40. Thomas, J.H.; Priyadarshini, G.; Michael, T. High-throughput micro plate assays for screening flavonoid content and DPPH-scavenging activity in sorghum bran and flour. *J Sci Food Agric* **2012,** *92*(11), 2326-2331. doi: 10.1002/jsfa.5633.
41. Luo-sheng, W.; Cui-ping, C.; Zuo-qi, X.; Yong-long, Wang; Qiu-xia, M.; Yuedong, Y.; Jiachun, C. In vitro and in vivo anti-diabetic activity of Swertia kouitchensis extract. *J Ethnopharmacol* **2013**, *147*(3), 622-630.
42. Nguyen, T.H.T.; Nguyen, T.V.; Tat, T.T.; Nguyen, T.T.G.; Nguyen, N.H.; Ho, H.T.D. (2007). Standardize the sulforhodamine B (SRB) test to determine the cytotoxicity of the natural compound. In Proceedings of National Scientific Conference 2007 - Basic Research in Life Sciences, Quy Nhon, Vietnam, 10/08/2007 (p. 809).
43. My-Nuong, T.N.; Thuy-Duong, H.-H. Selective cytotoxicity of a Vietnamese traditional formula, Nam Dia long, against MCF-7 cells by synergistic effects. *BMC Complement Altern Med* **2016**, *16*, 202-236.
44. Do, T.D. *Methods for determining acute toxicity of drugs;* Medical Publishing House, Ha Noi, Vietnam, 2014;